High-brightness AlGaInN light-emitting diodes

Krames, Michael, Christenson, G., Collins, Dave, Cook, Lou, Craford, M., et al.

Michael R. Krames, G. Christenson, Dave Collins, Lou W. Cook, M. George Craford, A. Edwards, Robert M. Fletcher, Nathan F. Gardner, Werner K. Goetz, William R. Imler, Eric Johnson, R. Scott Kern, Reena Khare, Frederick A. Kish, Chris Lowery, Mike J. Ludowise, Richard Mann, M. Maranowski, Steven A. Maranowski, Paul S. Martin, J. O'Shea, S. L. Rudaz, Dan A. Steigerwald, J. Thompson, Jonathan J. Wierer, Jingxi Yu, David Basile, Ying-Lan Chang, Ghulam Hasnain, M. Heuschen, Kevin P. Killeen, Christophe P. Kocot, Steven Lester, Jeffrey N. Miller, Gerd O. Mueller, Regina Mueller-Mach, S. Jeffrey Rosner, Richard P. Schneider Jr., Tetsuya Takeuchi, Tun S. Tan, "High-brightness AlGaInN light-emitting diodes," Proc. SPIE 3938, Light-Emitting Diodes: Research, Manufacturing, and Applications IV, (17 April 2000); doi: 10.1117/12.382822

SPIE.

Event: Symposium on Integrated Optoelectronics, 2000, San Jose, CA, United States

High-brightness AlGaInN light-emitting diodes

M. R. Krames, G. Christenson, D. Collins, L. W. Cook, M. G. Craford, A. Edwards, R. M. Fletcher, N. Gardner, W. Goetz, W. Imler, E. Johnson, R. S. Kern, R. Khare, F. A. Kish, C. Lowery, M. J. Ludowise, R. Mann, M. Maranowski, S. Maranowski, P. S. Martin, J. O'Shea, S. Rudaz, D. Steigerwald, J. Thompson, J. J. Wierer, J. Yu

LumiLeds Lighting, 370 W. Trimble Rd., San Jose, CA. 95131

D. Basile, Y-L Chang, G. Hasnain, M. Hueschen, K. Killeen, C. Kocot, S. Lester, J. Miller, G. Mueller, R. Mueller-Mach, J. Rosner, R. Schneider, T. Takeuchi, T. S. Tan

Agilent Laboratories, 3500 Deer Creek Road, Palo Alto, CA 94303

ABSTRACT

Currently, commercial LEDs based on AlGaInN emit light efficiently from the ultraviolet-blue to the green portion of the visible wavelength spectrum. Data are presented on AlGaInN LEDs grown by organometallic vapor phase epitaxy (OMVPE). Designs for high-power AlGaInN LEDs are presented along with their performance in terms of output power and efficiency. Finally, present and potential applications for high-power AlGaInN LEDs, including traffic signals and contour lighting, are discussed.

Keywords: LED, light-emitting diode, gallium nitride, high power LED, AlGaInN, InGaN

1. INTRODUCTION

The evolution of LED performance has proceeded at a phenomenal rate and is now at the point that these solid-state emitters are competing successfully against conventional lighting solutions in a number of applications. An illustration of the evolution of LED performance in commercial industry is shown in Fig. 1. The development of

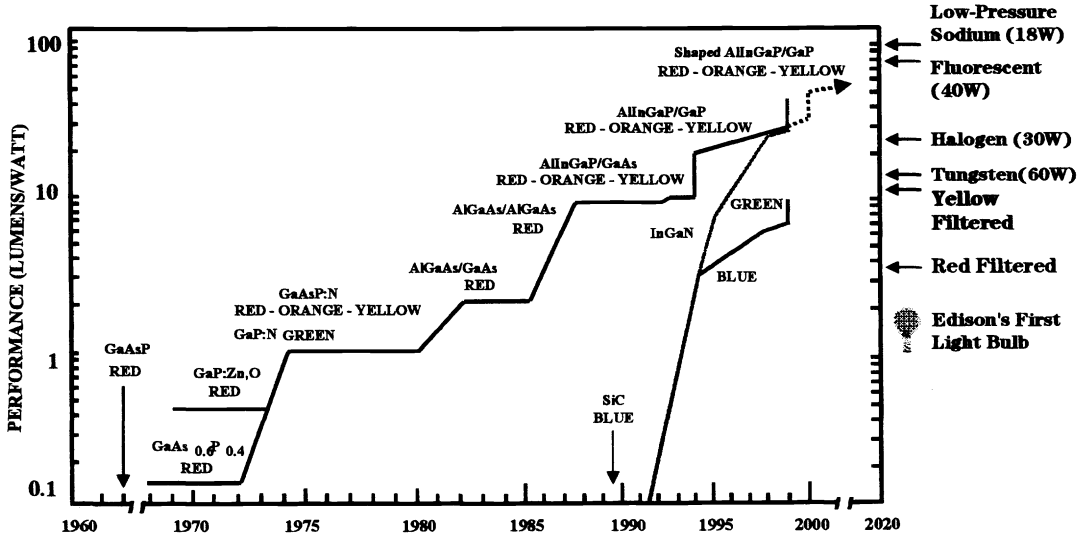

Fig. 1. The evolution of commercial LED performance and its comparison to conventional lighting technologies.

In *Light-Emitting Diodes: Research, Manufacturing, and Applications IV*, H. Walter Yao, Ian T. Ferguson, E. Fred Schubert, Editors, Proceedings of SPIE Vol. 3938 (2000) • 0277-786X/00/$15.00

compound semiconductor alloys and the demonstration of the first practical LED (red-emitting GaAsP) in 1962 provided the foundation for the commercial development of the solid-state lamp.[1] The discovery of the isoelectronic trap, nitrogen, in GaAsP in 1971 extended the useful wavelength spectrum of light-emitting diodes (LEDs) to the yellow spectral region.[2] A significant increase in the efficiency of red emitters was achieved through the development of AlGaAs/GaAs LEDs employing a fully lattice-matched direct bandgap system and heterostructure active regions.[3,4] In the 1970s the LED lamp exceeded the performance (luminous efficiency) of a red-filtered incandescent bulb. The performance of the AlGaAs LEDs was further improved by the development of transparent-substrate (TS) devices (AlGaAs/AlGaAs) which doubled the efficiency of these emitters compared to their absorbing-substrate (AS) counterparts.[5] The emergence of AlGaInP/GaAs technology in the 1980s extended the useful wavelength range of high-brightness emitters into the orange and yellow spectral regions.[6] The development of TS AlGaInP/GaP devices doubled the efficiency of these devices and demonstrated the commercial viability of direct compound semiconductor wafer bonding technology.[7] Additional improvements to both the internal and external quantum efficiency of TS AlGaInP/GaP devices using multi-well active region structures have resulted in devices with efficiencies >70 lm/W at a peak wavelength (λ_p) of 615 nm and external quantum efficiencies >30% at $\lambda_p \sim 632$ nm.[8] The utility of these devices as practical lighting sources has further been improved by the development of high-power, high-flux (10-20 lm) AlGaInP/GaP LED lamps.[9] Most recently, the employment of chip shaping to AlGaInP/GaP LED technology has resulted in power LEDs with luminous efficiencies exceeding 100 lm/W in the orange spectral region ($\lambda_p \sim 610$ nm), and external quantum efficiencies exceeding 55% in the deep red spectral region ($\lambda_p \sim 650$ nm)[10].

Similar dramatic improvements in LED performance have been achieved in the blue and green spectra region through the development of the AlGaInN material system. Photoluminescence from polycrystalline GaN was observed in 1962[11], and the first GaN-based LEDs were fabricated by material grown by hydride-phased vapor epitaxy (HVPE)[12-14]. The first GaN LEDs grown by OMVPE employed sapphire substrates and were demonstrated in 1984[15]. Considerable improvement was realized after the development of low-temperature buffer layers for high-quality GaN films[16] and the realization of p-type GaN:Mg using low-energy electron-beam ionization (LEEBI)[17]. In 1991, Nakamura and co-workers developed an annealing technique[18] that provided similar activation of Mg and subsequently demonstrated violet LEDs employing an InGaN active region[19]. The brightest AlGaInN LEDs are achieved using quantum-well active regions wherein the mole fraction of InN in the wells determines the peak emission wavelength[20]. Today, external quantum efficiencies of ~ 21% in the blue ($\lambda_p \sim 470$ nm) and ~ 15% in the green ($\lambda_p \sim 530$ nm) spectral regions have been observed. In photometric terms, these efficiencies correspond to ~10 lm/W and ~55 lm/W, respectively. The highest-reported luminous efficiencies of LEDs to date are shown in Fig. 2 and are dominated by the AlGaInN and AlGaInP material systems.

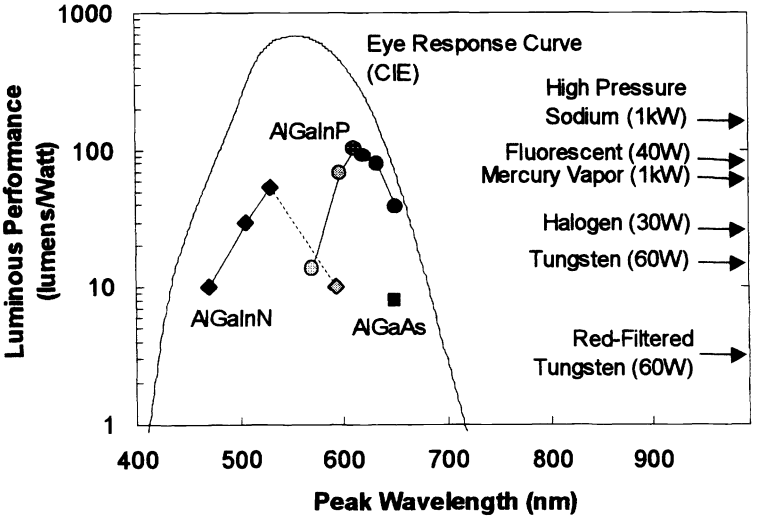

Fig. 2. Highest-reported LED luminous efficiencies.

2. STATUS OF III-NITRIDE LED TECHNOLOGY

The AlGaInN material system poses some unique challenges compared to conventional III-V material systems. Presently, the lack of a lattice-mismatched substrate results in very high defect densities, which, although not

strongly linked to poor quantum efficiency at the low current densities of LEDs, are nevetheless linked to reliability problems for AlGaInN laser diodes[21]. The two most common substrates used for OMVPE growth of AlGaInN are sapphire and SiC. Most commercial LED suppliers use sapphire substrates which are significantly less expensive than SiC. However, the use of sapphire as a growth substrate poses devices design challenges. Sapphire is insulating and therefore both p and n Ohmic contacts must be formed on the top surface of the LED chip. This is performed by mesa etching the AlGaInN LED structure to expose the n-type GaN layers beneath the active region. Ohmic n-contact metallization, typically Ti/Al, is applied to the n-type GaN. The p-type Ohmic contact is required to spread current from the p bond pad across the junction area because of the very low conductivity of GaN:Mg. This is typically done by depositing a semi-transparent Ni/Au Ohmic contact metallization across the GaN:Mg surface. Current from the n-type contact is required to spread through the GaN:Si layers beneath the active region. A typical device structure is shown in Fig. 3. In general, this type of structure results in an increased series resistance compared to LEDs based on other III-V material systems, and provides a challenge in terms of achieving the highest possible power conversion efficiencies.

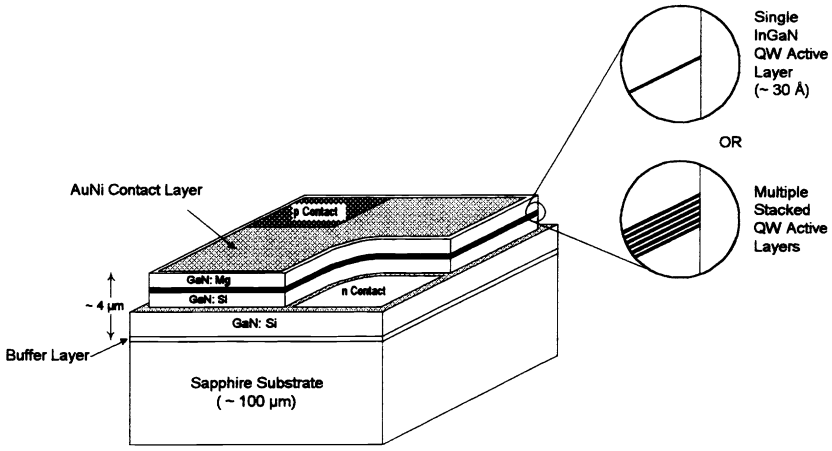

Fig. 3. Typical AlGaInN LED structure.

Even accounting for the increased series resistance, AlGaInN LEDs presently exhibit higher forward voltages than LEDs in other III-V material systems. Figure 4 shows a plot of forward voltage (at 20 mA) vs. bandgap energy for LEDs based on several different material systems. It is notable that AlGaInN LEDs throughout the blue, green, and amber sprectral regions exhibit forward voltages about 0.5-1.0 V higher than their bandgap voltages. A comparison of current-voltage characteristics of AlGaInP and AlGaInN LEDs, shown in Fig. 4b, show that this voltage increase is apparent at very low current levels. At 1 mA, the AlGaInP LED exhibits a forward voltage of 1.8V, about 300 mV below the bandedge emission at 593 nm. At the same current, the AlGaInN LED exhibits a forward voltage of 2.4 V, which is only about 80 mV below the bandedge emission for 500 nm. The difference in series resistance between the two structures is, worst case, about 20 Ω. At 1 mA, the difference in series resistance can only account

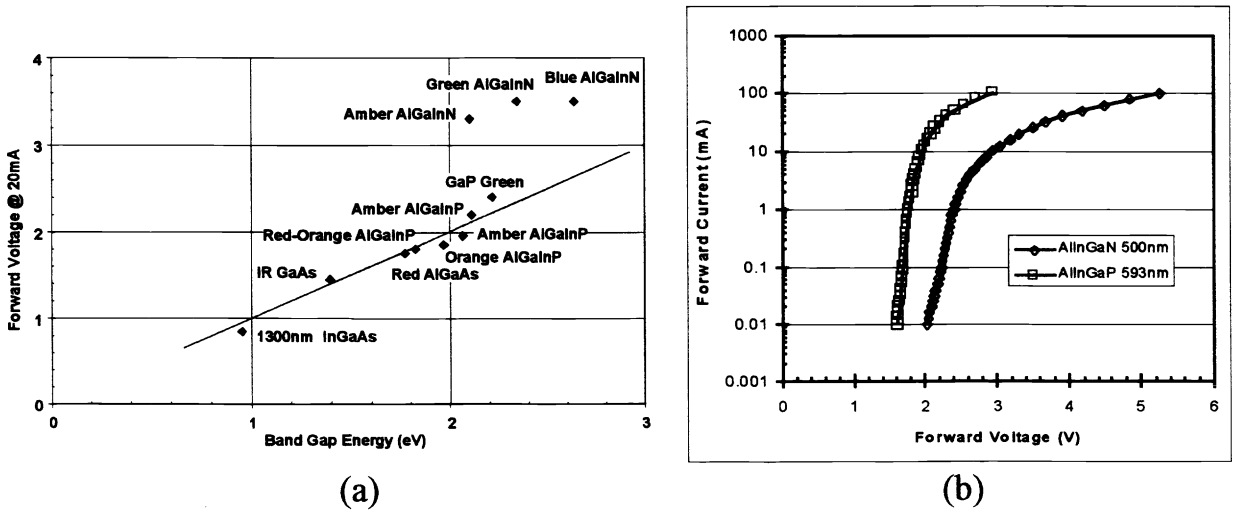

(a) (b)

Fig. 4. (a) Comparison of forward voltage characteristics of AlGaInN LEDs compared to LEDs based on other III-V materials systems. (b) Comparison of current-voltage charactersistics between an AlGaInP LED (593 nm) and a AlGaInN LED (500 nm).

for 20 mV of the difference in forward voltage. Thus, the AlGaInN LED has additional ~200 mV forward voltage increase at 1mA compared to the AlGaInP LED. At 20 mA, the same comparison yields ~ 400 mV of increased voltage (offset) for the AlGaInN LED. Presumably, the increased forward voltage for the AlGaInN LEDs are due to internal barriers to conduction through the p-n junction heterostructure. The heterostructure designs are typically comprised of InGaN quantum wells with GaN or InGaN barriers, surrounded by GaN confining layers. An AlGaN "electron stopper" layer is usually provided on top of the active region to improve electron confinement. This type of design, coupled with piezoelectric effects and spontaneous polarization fields on the band structure, may be responsible for the increased forward voltages observed in today's AlGaInN LEDs.

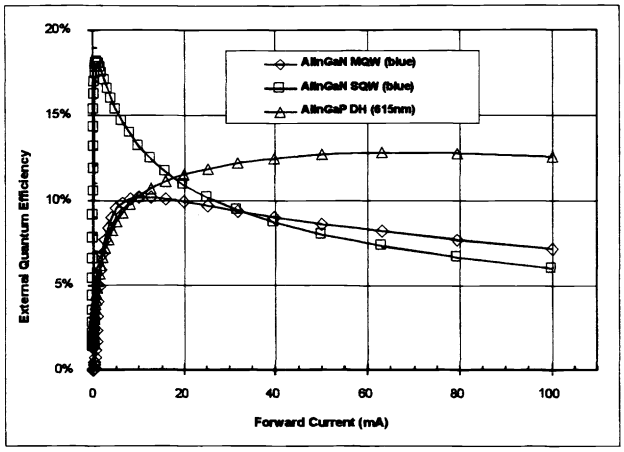

Fig. 5. External quantum efficiency of single- and multiple-quantum-well AlGaInN LEDs as function of current density, as compared to AlGaInP.

AlGaInN LEDs also differ from conventional III-V LEDs in terms of quantum efficiency as a function of current density. Figure 5 compares single- and multiple-quantum-well AlGaInN LED structures with a AlGaInP double-heterostructure LED. The AlGaInP LED exhibits increased quantum efficiency with increasing current density, until carrier leakage and thermal effects limit the maximum achievable efficiency. For the AlGaInN LEDs, the quantum efficiency peaks at low currents and decreases with increasing current density. This is especially apparent for the single-quantum-well structure, whose peak efficiency at ~1mA is 1.7x higher than that at 20 mA. For the multiple-quantum-well structure, the effect is less pronounced. Even so, the reduced quantum efficiency at higher current levels (e.g., 50 mA) for AlGaInN poses a challenge for realization of high-flux LEDs with high power-conversion efficiency. The details of the recombination physics in InGaN-GaN-AlGaN active regions needs to be better understood in order to provide a model for the decreased efficiency at high current levels and to provide hope for solving this problem.

Another issue with AlGaInN LEDs is obtaining a stable emission spectrum. Especially at long wavelengths, the electroluminescence peak shifts to shorter wavelengths with increasing current density. The effect is illustrated in Fig. 6. Blue AlGaInN LEDs at ~ 470 nm exhibit only a ~5 nm shift in going from 1 to 100 mA drive current. A "green" AlGaInN LED shifts from ~520 nm to ~ 505 nm over the same current range. Finally, an "amber" AlGaInN LED exhibits a very large FWHM, and shifts from ~595 nm to ~550 nm. Clearly the "amber" AlGaInN LED is no longer "amber" at the higher drive current. Even in going from 1 to 10 mA, the "amber" AlGaInN LED spectrum has shifted to the yellow spectral region. This problem makes the realization of long-wavelength AlGaInN LEDs difficult, since color control and stability provide enormous yield problems in high-volume manufacturing. Also, for AlGaInN emitters at wavelengths greater than $\lambda_p \sim$ 470 nm, the quantum efficiency decreases significantly with increased In composition in the active region. Further development is necessary before AlGaInN LEDs can realistically compete

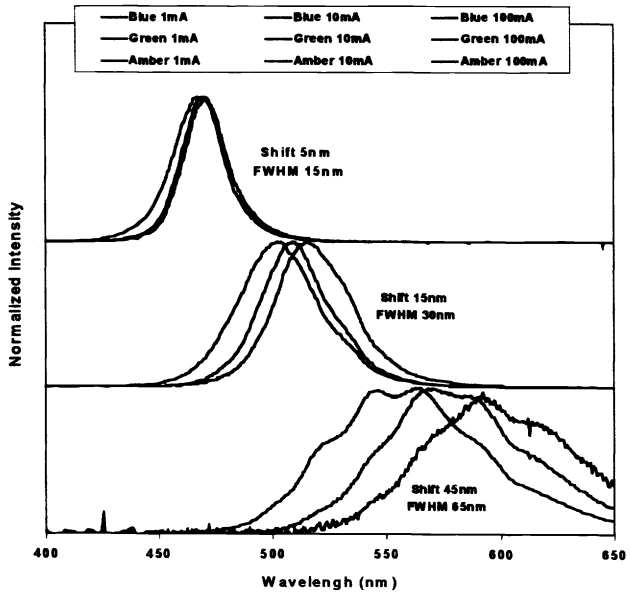

Fig. 6. Electroluminescence of blue, green, and "amber" AlGaInN LEDs at forward current levels of 1, 10 and 100 mA.

with AlGaInP LEDs in the yellow-amber wavelength regime.

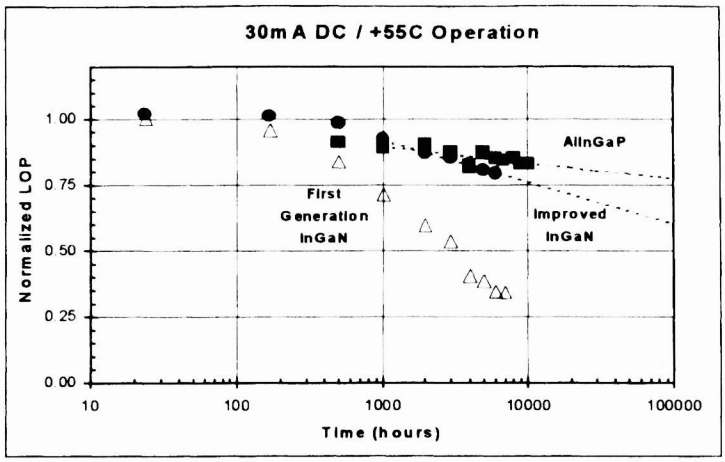

Fig. 7. Reliability performance of both "first-generation" and "improved" AlGaInN LEDs, as compared to AlGaInP.

Another serious issue for AlGaInN LED performance is reliability. Initial AlGaInN LED reliability was fairly poor, with a significant drop in light output observed under high-temperature operating lifetime tests beyond 500 hrs. Further investigation showed that the root cause of the degradation was due to the package, and not the LED chip[22]. By replacing the clear die-attach epoxy used to mount the LED chip to the lead-frame with a Ag-loaded die-attach epoxy, AlGaInN LED reliability was dramatically improved. Unfortunately, the switch to Ag-loaded die-attach epoxy resulted in a decrease in light output, presumably because of the poor reflectivity of this epoxy. By inserting a metal back-reflector on the sapphire substrate, the light output was recovered to result in a reliable AlGaInN LED with no penalty to light output. A summary of reliability characteristics of "first generation" and "improved" AlGaInN LEDs is shown in Fig. 7, along with a typical AlGaInP LED reliability characteristic for comparison. Presently, the best AlGaInN LED reliability performance begins to approach that of typical AlGaInP reliability at the same current density and junction temperature.

3. HIGH-POWER III-NITRIDE LEDS

In order to compete effectively with conventional light sources, solid-state lamps based on LEDs must have comparable flux levels. Unfortunately, standard 5mm LED lamps driven at 20-30 mA only provide a few lumens of flux, in contrast to the many hundreds or thousands produced by conventional light sources. This disparity makes it difficult for LEDs to compete with conventional solutions in many applications. For example, in order to provide the same level of flux as a 60W incandescent light bulb, a solid-state light source would require several hundred LEDs. The required large number of packages increases assembly cost and real estate. Furthermore, the high thermal resistance of 5mm lamp packages limits the drive current and thus the total available flux that the LED chips can provide. By increasing the chip size and providing low-thermal-resistance power packages capable of dissipating several Watts, LEDs should be able to compete more favorably with conventional lighting technologies in many applications.

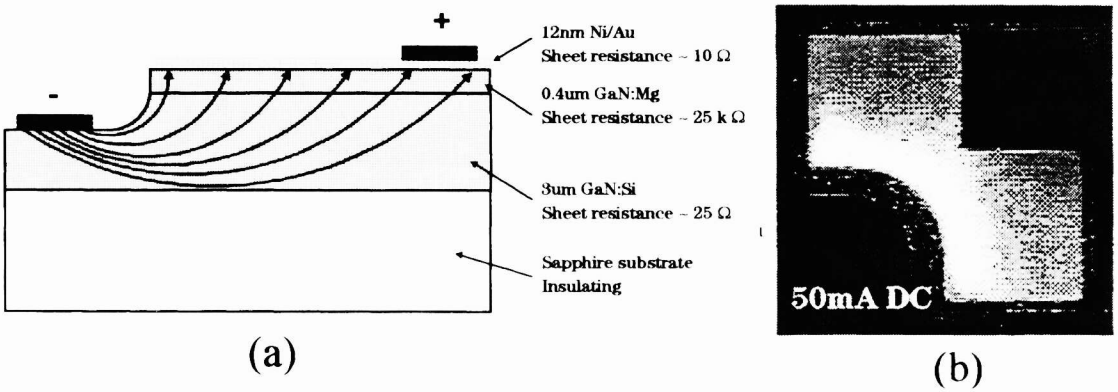

Fig. 8. (a) Sheet resistances in a typical AlGaInN LED structure. (b) Lit visual of AlGaInN LED at 50 mA, showing current crowding towards the n-type Ohmic contact.

In order to provide a power LED chip, the junction area must be increased to accommodate the larger input power. To spread current uniformly throughout the p-n junction for a large-area LED, the Ohmic contacts must be re-configured. The exact configuration will effect the series resistance of the device which is governed by the sheet resistances of the various layers of the AlGaInN LED structure. Typical values for these sheet resistances are shown in Fig. 8a. For a device with a typical Ni/Au p Ohmic contact (~10 Ω), the current spreading is limited not by this layer but by the GaN:Si layer instead (~25 Ω). This discrepancy suggests that it is current spreading from the n Ohmic contact that will be the dominant cause of current crowding at higher current densities. Indeed, this is observed in conventional device designs at high currents as illustrated in Fig. 8b, where light is generated at the n-contact due to crowding.

Clearly, a power AlGaInN LED requires an improved contact configuration in order to avoid the current crowding problem illustrated in Fig. 8b. Also, it is important that series resistance be kept to a minimum. A typical AlGaInN LED design like that shown in Fig. 8b has a series resistance of 20-30 Ω. Typical values for AlGaInP (vertical-injection) LEDs are 5-10 Ω. Improvement in an AlGaInN LED structure is evident in a new design, illustrated in

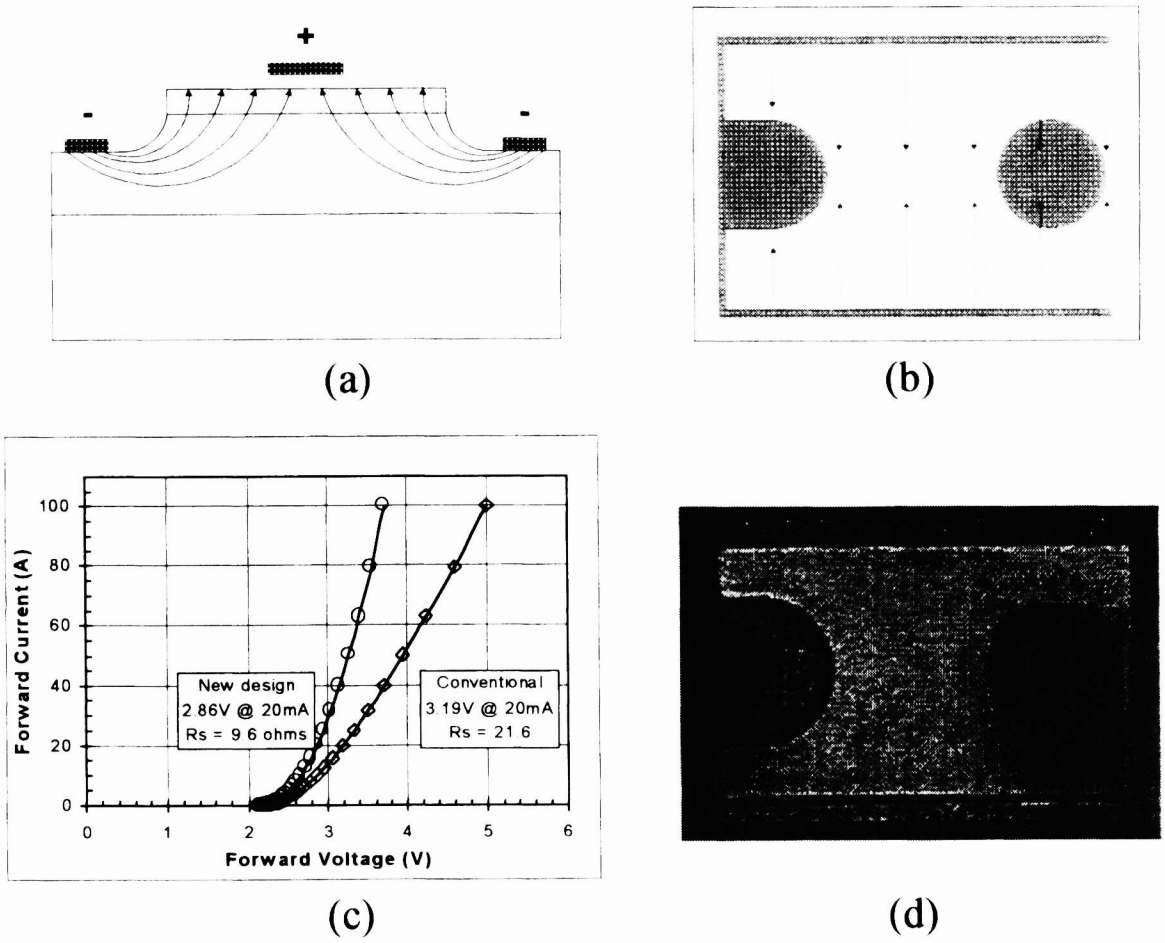

Fig. 9. (a) Cross-sectional and (b) plan views of improved AlGaInN LED structure. (c) Current-voltage characteristic of improved AlGaInN structure, as compared to the conventional device. (d) Lit visual of the improved structure at 50 mA.

Fig. 9. Figure 9a shows a schematic cross-section of an improved AlGaInN LED design, wherein the n Ohmic contact is brought along either side of the GaN:Mg mesa to reduce the spreading distance required by the current in the GaN:Si layers. A plan view of the device is shown in Fig. 9b. Such devices were fabricated and their current-voltage characteristics were measuread and compared to those of standard AlGaInN LED structures from the same wafer. The results are shown in Fig. 9c. The improved design provides a series resistance of ~ 9.6 Ω at 20 mA, less than half that of the conventional design (21.6 Ω). The effect is dramatic at high currents: at 100 mA the improved

design exhibits a forward voltage of 3.6 V as compared to 5.0 V for the conventional structure. A lit visual of the improved LED at 50 mA is shown in Fig. 9d, which does not exhibit current crowding effects such as shown in Fig. 8b.

The above improved contact configuration can be extended to power AlGaInN LED design. This concept is illustrated in Fig. 10. By having interdigitated n and p Ohmic contacts, a large area LED may have excellent current spreading capability and low series resistance, both of which are very important for high-power operation. Figure 10a shows a plan view schematic of a 1x1 mm^2 AlGaInN LED chip employing an interdigitated contact design. Figure 10b shows a schematic of the same structure in cross section. Each set of p Ohmic contacts is surrounded by two n Ohmic contact fingers, comprising a "cell" with a certain electrical resistance. By combining these cells as demonstrated in Fig. 10a and b, the total resistance of the device is the resistances of these cells in parallel. Therefore, the more cells in the design, the lower the series resistance.

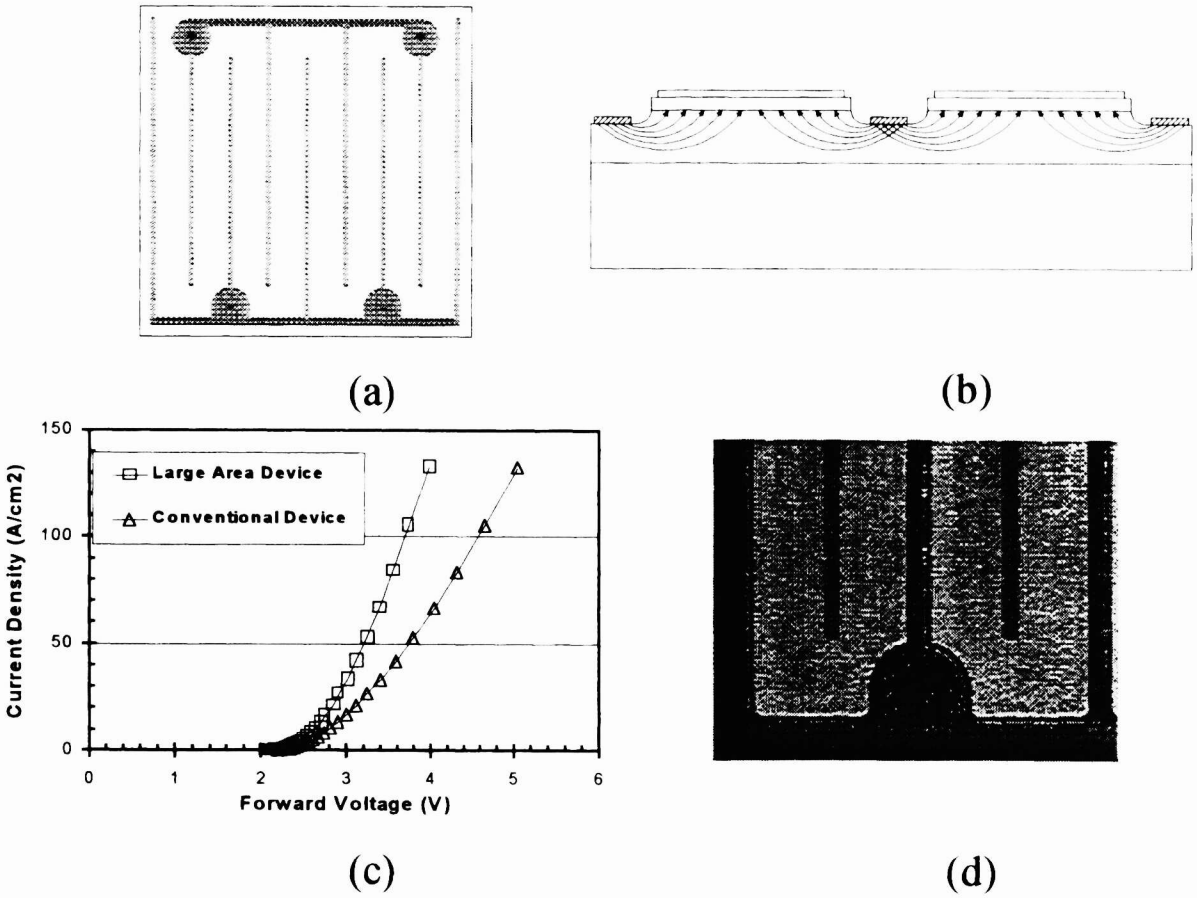

Fig. 10. (a) Cross-sectional and (b) plan views of a 1x1 mm^2 power AlGaInN LED structure. (c) Voltage as a function of current density of the power AlGaInN LED, as compared to the conventional device (~ 0.35 x 0.35 mm^2). (d) Lit visual of a portion of the power AlGaInN LED at 350 mA.

A simple calculation shows that the series resistance of the LED is proportional to N^{-2}, where N is the number of cells. Experimental optimization for the 1x1 mm^2 device at 350 mA shows that four cells achieves the best performance in terms of power conversion efficiency. The forward voltage of such an LED is plotted in Fig. 10c as a function of current density, along with that of a conventional AlGaInN LED structure (~ 0.35 x 0.35 mm^2). The power AlGaIN LED is shown to have an improved electrical performance even though it contains roughly ten times the junction area of the conventional device.

One drawback of the power AlGaInN LED with respect to the conventional structure is with respect to light extraction efficiency. Experimental measurements of external quantum efficiency as a function of junction area consistently show a decrease in quantum efficiency with increasing junction area. This is illustrated in Fig. 11 for die sizes from 0.5 to 1.5 mm. The quantum efficiencies are normalized to the case for a conventional 0.35 mm size AlGaInN LED. The reduction in quantum efficiency is significant, with a ~25% decrease observed between the 0.35 and 1.0 mm cases. Ray-trace modeling of AlGaInN LEDs indicates that this reduction in quantum efficiency is due to decreased extraction efficiencies for the large-area LEDs. For these LEDs, the low aspect ratio prevents much of the light from escaping out the sides of the chip. This light is instead bounced around inside the chip and is susceptible to reabsorption at many of the optical loss mechanisms present, such as free-carrier or Ohmic contact absorption. Interestingly, the same phenomenon is observed for AlGaInP, suggesting that this is strictly an issue of geometry. In fact, as shown in Fig. 11, the AlGaInP efficiency derating with increased junction area does not differ appreciably from that of AlGaInN LEDs.

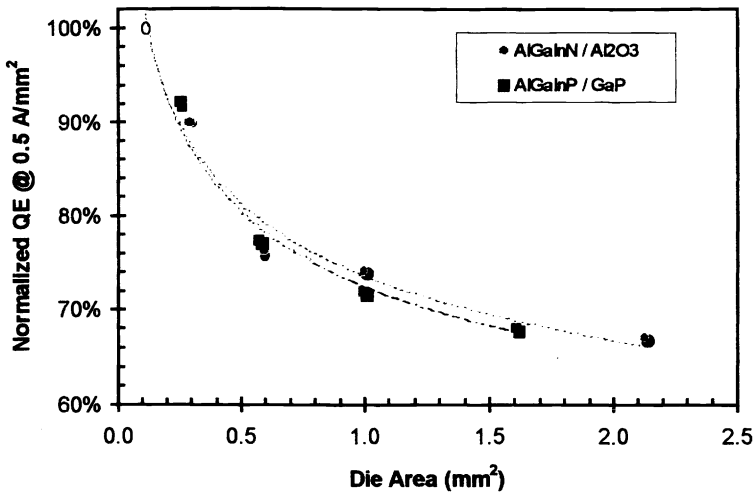

Fig. 11. Normalized external quantum efficiency vs. die area for both AlGaInN and AlGaInP LEDs.

In order to derive full light-generating capability from the power AlGaInN LED chip, a high-power, low thermal resistance package is required. Recently, a power package for AlGaInP power LED chips has been demonstrated[9]. This package can dissipate several Watts of power and inserts a thermal resistance of only 2°C/W. The Cu body provides good heat-sinking while a two-part lens is comprised of a hard outer lens and a soft, low-stress inner encapsulant.

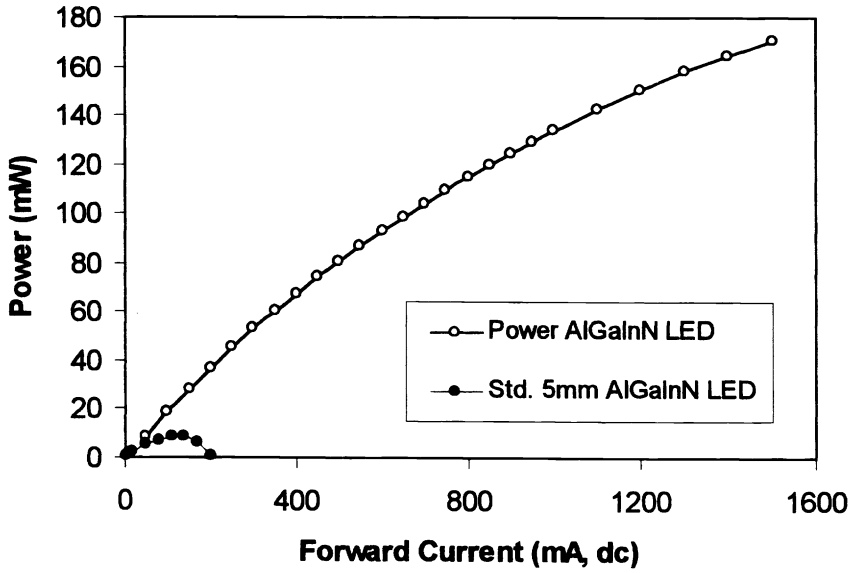

Fig. 12. Light output vs. current characteristic of a blue (λ_p ~470 nm), 1x1 mm^2 AlGaInN LED in a power package, compared to a conventional AlGaInN LED in a 5 mm lamp package.

The light output vs. current characteristic for a blue (λ_p ~470 nm), 1x1 mm^2 AlGaInN LED mounted in a power package is shown in Fig. 12. A power output of over 170 mW is obtained at a drive current of 1.5 A dc. The fact that the output power has not saturated at 1.5 A is a tribute to the excellent thermal characteristics of the power package and the low temperature dependence of quantum efficiency for the AlGaInN LED. For comparison, a conventional AlGaInN LED (~0.35x0.35 mm^2) with similar quantum efficiency in a 5 mm lamp package exhibits a peak output power of less than 10 mW at 100 mA. A summary of the performance characteristics of a cyan (λ_p ~ 505 nm) power AlGaInN LED as compared to the conventional device are summarized in Table I for equivalent current densities (~ 45 A/cm^2).

The heat dissipating capability of the power package, coupled with the low-stress inner encapsulant surrounding the chip, allow for excellent reliability performance of the high-power AlGaInN LED. Typical reliability performance for the high-power LEDs under high-temperature operating lifetime tests are shown in Fig. 13. At 350 mA (~ 1 W), the power AlGaInN LEDs exhibit excellent reliablity performance, with projected degradation less than 20% out to 100,000 hrs. Referring to Fig. 7, the power LEDs exhibit improved performance compared to the case for conventional LEDs for the same current density (30 mA). Reasonable reliability performance is observed for the power LEDs at much higher current densities. At 1.0 A (~ 4 W) operation, the projected half-power liftetime is ~ 100,000 hrs. This performance is comparable to that for the conventional devices at 30 mA, but at more than 30 times the forward current!

Table I. Typical performance characteristics of high-power AlGaInN LEDs in power packages compared to conventional devices in 5 mm lamps (λ_p ~ 505 nm).

Drive Current	30 mA	350 mA
Forward Voltage	3.6 V	3.3 V
Input Power	0.1 W	1.1 W
Thermal resistance	~ 300 C/W	~ 12 C/W
Junction Temperature Rise	+ 30 C	+ 13 C
Flux	1-2 lm	10-15 lm

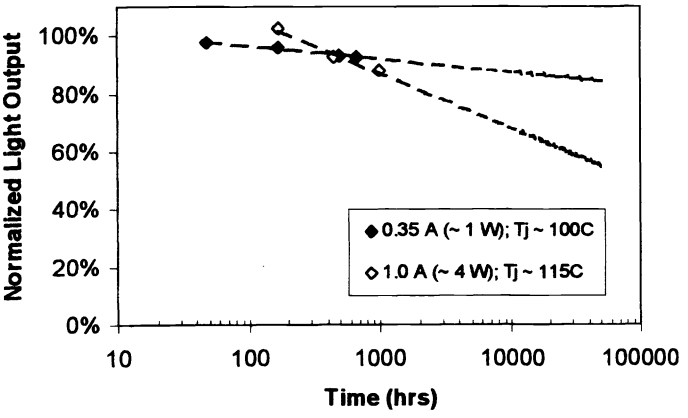

Fig. 13. High-temperature operating lifetime stress of power AlGaInN LEDs at forward currents of 0.35 and 1.0A.

4. APPLICATIONS

The high power AlGaInN LEDs enable applications wherein high flux density is important, and offer advantages over solutions employing conventional LEDs. An example of one application where high-flux LEDs offer unique advantages is traffic signaling. The advent of power LEDs has allowed the reduction in the number of LEDs required for a traffic ball from a few hundred down to just 12 to 18. This reduction in the required number of emitters is illustrated in Fig. 14. This allows the lighting engineer to treat the LEDs as a compact, high-flux light source in the design of the traffic ball. Through the use of secondary optics, the desired radiation pattern for the traffic signal application is achieved. Moreover, unlike for the case of conventional LEDs which can appear "spotty", the high-flux light engine mated with secondary optics results in an extremely uniform appearance of the radiance across the traffic ball.

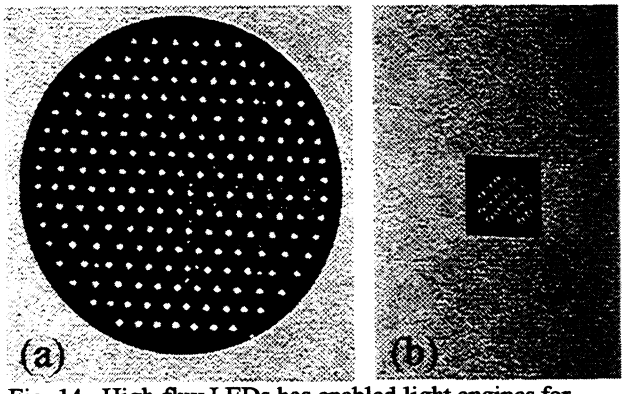

Fig. 14. High-flux LEDs has enabled light engines for traffic balls to reduce LED count from (a) a few hundred, to (b) eighteen.

One application that high-flux LEDs enable is lighting via fibres. The flux densities required for efficient lighting via fibres are not achievable using conventional LEDs. This is not the case for power LEDs, which offer more than ten times the flux in roughly the same area. A schematic cross-section of a power LED fibre light engine is shown in Fig. 15a along with a prototype module in Fig. 15b.

The possible applications for LED fibre light engines are many. Because they are solid state, the LED fibre engines are small, compact, and efficient, and do not require a cooling fan as is the case for fibre light engines using conventional light sources. Also, different color LEDs may be mixed in the light engine module to provide a wider variety of colors, even white. These colors may even be externally controlled to provide dynamic color changes for certain applications. Also, the LED fibre engine will benefit from the long-life of solid-state emitters. Finally, the system is actually cheaper to manufacture than its conventional counterpart.

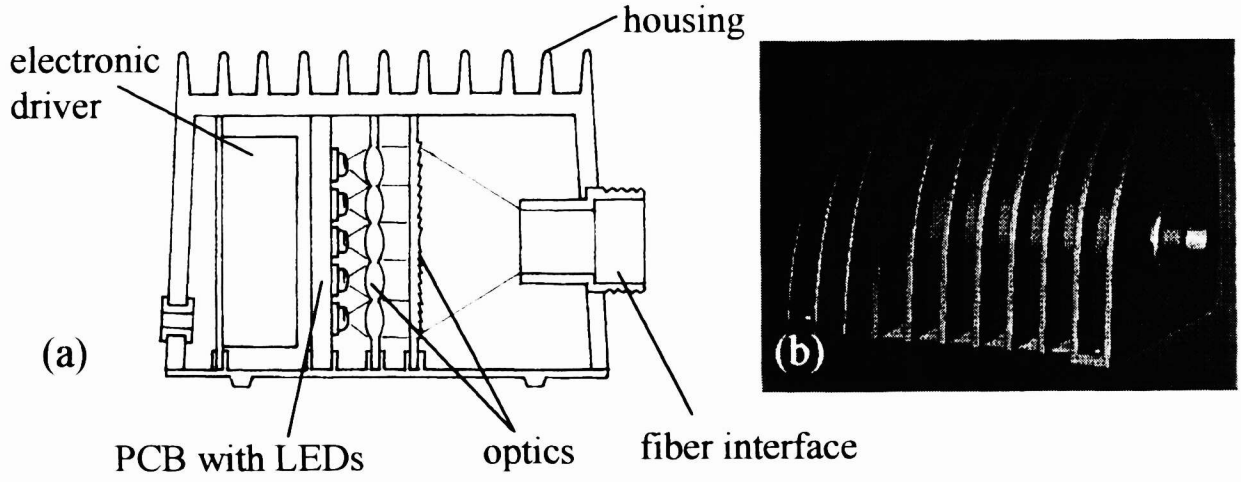

Fig. 15. Power LED fibre light engine: (a) schematic cross-section, and (b) photograph of prototype module.

5. CONCLUSIONS

There are of course many other applications suitable for the use of power AlGaInN LEDs. The conversion of blue light into white via phosphors enables power AlGaInN LEDs to produce several lumens of white light per emitter, such that one can envision a white flashlight which is comprised of only one LED and which draws less power than an incandescent bulb. As penetration into existing applications increases, and new applications emerge, solid-state light emitters will continue to increase their value proposition to the world, offering more lumens for reduced cost. Similarly, continued research and development of these material systems will yield more efficient and higher power LEDs, resulting in emitters with increased luminous output. This trend has been going on since the invention of the LED. Figure 16 illustrates this for red emitters, which have the longest history. The trend in cost reduction is dramatic, with ten-fold reduction in cost per lumen per decade. Similarly, the increase in lumens per emitter is

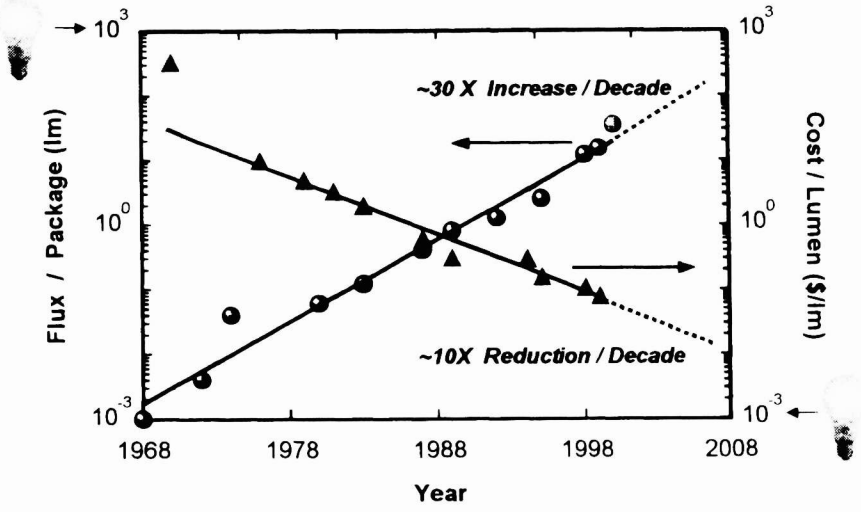

Fig. 16. The evolution of red LED technology in terms of cost and flux.

increasing at an incredible ~ 30x per decade. At these rates, the LED will catch up with the conventional light bulb in terms of cost and power in the early part of the 21st century, and penetrate the last vestiges of the lighting market now served by conventional lighting technologies.

ACKNOWLEDGEMENTS

The authors would like to acknowledge several people who contributed to this work, including: B. Kock and H. Konijn, at LumiLeds Lighting b.v. in Best, the Netherlands; A. Seppen-Saalberg, G. Harbers, and B. Hontele, at Philips Lighting in Eindhoven, the Netherlands; P. Arellano, C. Bautista, A. Davis, N. Felmoca, D. Patterakis, A. Rin, and J. Wood, at LumiLeds Lighting in San Jose, California.

REFERENCES

1. N. Holonyak, Jr.and S.F. Bevaqua, *Appl. Phys. Lett.* **1**, 82-83 (1962).
2. W.O. Groves, A.H. Herzog and M.G. Craford, *Appl. Phys. Lett.* **19**, 184 (1971).
3. H. Rupprecht, J.M. Woodall and G.D. Petit, *Appl. Phys. Lett.* **11**, 81-83 (1967).
4. J. Nishizawa, K. Suto and T. Teshima, *J. Appl. Phys.* **48,** 3484-3495 (1977).
5. H. Ishiguro, K. Sawa, S. Nagao, H. Yamanaka and S. Koike , *Appl. Phys. Lett.* **43**, 1034-1036 (1983).
6. C.P. Kuo, R.M. Fletcher, T.D. Osentowski, M.C. Lardizabal, M.G. Craford and V.M. Robbins, *Appl. Phys. Lett.* **57**, 2937-2939 (1990).
7. F.A. Kish, F.M. Steranka, D.C. DeFevere, D.A. Vanderwater, K G. Park, C.P. Kuo, T.D. Osentowski, M.J. Peanasky, J.G. Yu, R.M. Fletcher, D.A. Steigerwald, M.G. Craford and V.M. Robbins, *Appl. Phys. Lett.* **64,** 2839-2841 (1994).
8. N.F. Gardner, H.C. Chui, E.I. Chen, M.R. Krames, J.-W. Huang, F.A. Kish, S.A. Stockman, C.P. Kocot, T.S. Tan and N. Moll, *Appl. Phys. Lett.* **74**, 2230-2232 (1999).
9. G.E. Hofler, C. Carter-Coman, M.R. Krames, N.F. Gardner, F.A. Kish, T.S. Tan, B. Loh, J. Posselt, D. Collins and G. Sasser, *Electron. Lett.* **34**, 1781-1782 (1998).
10. M.R.Krames, M.Ochiai-Holcomb, G.E.Hofler, C.Carter-Coman, E.I.Chen, I.-H.Tan, P.Grillot, N.F.Gardner, H.C.Chui, J.-W.Huang, S.A.Stockman, F.A.Kish, M.G.Craford, T.S.Tan, C.P.Kocot, M.Hueschen, J.Posselt, B.Loh, G.Sasser, D.Collins, *Appl. Phys. Lett.* **75**, pp. 2365-2367 (1999).
11. M.R.Lorenz and B.B.Binkowski, *J. Electrochem. Soc.* **109**, 24 (1962).
12. H.P.Maruska and J.J.Tietjen, *Appl. Phys. Lett.* **15**, 327 (1969).
13. J. I.Pankove, E.A.Miller, D.Richman, and J.E.Berkeyheiser, *J. Lumin.* **4**, 63 (1971).
14. H.P.Maruska, W.C.Rhines, and D.A.Stevenson, *Mater. Res. Bull.* **7**, 777 (1972).
15. T. Kawabata, T.Matsuda, and S. Koike, *J. Appl. Phys.* **56**, 2367 (1984).
16. H.Amano, N.Sawaki, I.Akasaki, and Y.Toyoda, *Appl. Phys. Lett.* **48**, 353 (1986).
17. H.Amano, M.Kito, K.Hiramatsu, N.Sawaki, and I. Akasaki, *Jpn. J. Appl. Phys.* **28**, L2112 (1989).
18. S.Nakamura, M.Senoh, and T.Mukai, *Jpn. J. Appl. Phys.* **30**, L1708 (1991).
19. S.Nakamura, T.Mukai, M.Senoh, S.Nagahama, and N.Iwasa, *J. Appl. Phys.* **74**, 3911 (1993).
20. S.Nakamura, M.Senoh, N.Iwasa, and S.Nagahama, *Jpn. J. Appl. Phys.* **34**, L797 (1995).
21. S.P.DenBaars, M.A.Hansen, H.Marchand, G.Parish, P.Fini, T.Katona, M.Craven, U.K.Mishra, to be published in *Proceedings of SPIE* Vol. 3938 (2000).
22. D. A. Steigerwald, *Proceedings of the 2nd International Conference on Nitride Semiconductors,* 514 (1997).